

Chapter 4

Modelling Emulsion Polymerisation for Large Particles

*All theoretical chemistry is really physics;
and all theoretical chemists know it.*

– Richard P. Feynman

As discussed in section 3.3, an emulsion polymerisation recipe may lead to a polydisperse particle size distribution (PSD) or even a bimodal PSD if new nucleation occurs. To assist the development of a recipe for the synthesis of large polymer particles, a model of the particle formation process was developed. The principal aim of this model was to determine whether or not a set of experimental conditions would successfully produce a large sized latex, but not necessarily to accurately quantify any failure. This important condition on the model permits several simplifications to be made as detailed below.

The model was based on previous work by Morrison *et al.*¹ and has been tailored to the polymerisation of styrene with a persulfate initiator, as previous experimental work indicates that micron-sized polystyrene particles may be synthesised by emulsion polymerisation.²⁻⁴

4.1 Kinetics of Emulsion Polymerisation

The kinetics of particle formation and particle growth in emulsion polymerisation are a complex interplay between chemical and physical events. These processes have been successfully described in terms of kinetic equations,⁵ which have been used to construct predictive models of the particle size distributions^{6,7} and molecular weight distributions⁸ that result from emulsion polymerisation experiments.

There are three principal events that must be adequately described to successfully model emulsion polymerisation. These are the formation of new particles, the reactions of aqueous phase radicals and the growth of the particles.

The mathematical description adopted in this work is an extension of previous work that was shown to successfully reproduce secondary nucleation quantification experiments.¹ Some of the processes included in more complete descriptions of emulsion polymerisation⁶ were not included in this model as they were too computationally expensive to be employed in a study to find conditions to grow large

particles. For completeness, these processes are briefly described in the appendices and the simplifications in the model and their repercussions are identified in section 4.2.1.

4.1.1 Kinetics of Particle Formation

Within the description of how particles form in emulsion polymerisation there are four principal processes that vary in significance according to the reaction parameters of the system.⁵ These are homogeneous, micellar and droplet nucleation and the coagulation of existing particles. Of these, homogeneous nucleation is the only process included here. This simplification is discussed further in section 4.2.1. A brief discussion of the three processes omitted may be found in Appendix 1.

4.1.1.1 Homogeneous Nucleation

As described in section 3.3, an aqueous phase oligomeric radical derived from an initiator fragment may reach the critical degree of polymerisation for chain collapse, j_{crit} , at which point the chain becomes swollen with monomer and becomes a particle.⁵ This has also been described as a rapid rod-to-coil transition called a “precipitation”.⁵ The rate of formation of j_{crit} -mers may be described as follows:⁵

$$\frac{d[\text{IM}_{j_{\text{crit}}}^{\bullet}]}{dt} = k_{\text{p,aq}}^{j_{\text{crit}}-1} [\text{IM}_{j_{\text{crit}}-1}^{\bullet}] C_w \quad (4.1)$$

where $k_{\text{p,aq}}^{j_{\text{crit}}-1}$ is the aqueous phase chain propagation rate coefficient of a $(j_{\text{crit}}-1)$ -mer and C_w is the monomer concentration in the aqueous phase.

This transition occurs when the charged initiator fragment is no longer able to solubilise the growing hydrophobic polymer chain. Values for j_{crit} have been estimated from the comparison of solvation energies for sulfonated surfactants analogous to the polymeric radicals being described.^{5,9} Additionally, j_{crit} may be estimated from thermodynamic arguments:^{5,9}

$$j_{\text{crit}} = 1 - \frac{55 \text{ kJ mol}^{-1}}{RT \ln C_{\text{w}}^{\text{sat}}} \quad (4.2)$$

where $C_{\text{w}}^{\text{sat}}$ is the saturation concentration of monomer in the aqueous phase measured in mol dm^{-3} , T is the temperature and R the gas constant. However, the kinetic validity of this relationship remains unclear.⁵

Once this transition has occurred, the coil is able to swell with more monomer, allowing further propagation of the chain. This collapsed, swollen chain is considered to be a particle,^{5,9-11} as its growth is now governed by the particle growth kinetics described in section 4.1.3.

The amount of nucleation that occurs in any system through this method is determined by the longevity of the aqueous phase polymeric radicals in the system. Reducing the concentration of aqueous phase initiator fragments with degrees of polymerisation 1 to $j_{\text{crit}}-1$ reduces the possibility of homogeneous nucleation occurring. This may be achieved through aqueous phase processes such as termination or by phase changes such as particle entry as discussed in section 4.1.2.

4.1.2 Kinetics of Aqueous Phase Radicals

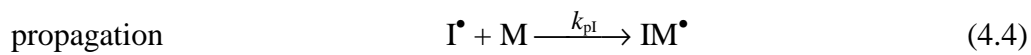
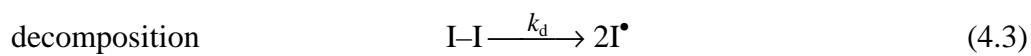
The generation, propagation and termination of aqueous phase radicals has a profound impact on the emulsion polymerisation process. Aqueous phase radicals are predominantly derived from initiator fragments, although it is possible for monomeric radicals formed by chain transfer to monomer events (see section 3.3) to take part in aqueous phase reactions.

4.1.2.1 Steady State Calculations of Radical Concentrations

As described in section 3.3, the decomposition of initiator forms radicals that may react with aqueous monomer. For many common initiators (such as potassium persulfate) the decomposition process forms two identical radicals. Since decomposition is slow and the species under consideration are quite reactive, their

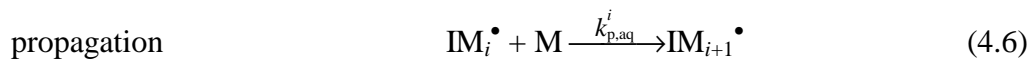
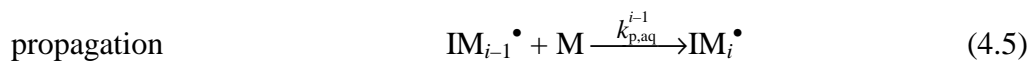
concentrations are typically quite low and thus the steady state approximation may be used in determining the concentration of the initiator fragments.^{5,9} Moreover, the complex dependencies between the concentrations may be computationally simplified using an iterative process.⁵

In the description of these reactions, it is assumed that the decomposed initiator radicals, I^\bullet , will have propagated before they are able to undertake termination reactions with other radical species. Thus the reactions involved at this stage are:



Previous studies have shown that the termination and propagation rate coefficients for the I^\bullet to be quite similar in magnitude;^{5,9} however the concentration of monomer in the aqueous phase is typically orders of magnitude greater than the concentration of radicals. Termination of the I^\bullet species is thus considered to be negligible.

The concentration of oligomeric radicals of degree of polymerisation 1 to $z-1$ (i.e. non-surface active species) may be derived from the following reaction scheme:



where reaction 4.7 describes radical recombination or disproportionation reactions resulting in the termination of the radical with rate coefficient $k_{t,aq}$. In line with previous work,⁹ it is assumed that this rate coefficient is not dependent on the length of the chains involved and may thus be interpreted as an “average” rate coefficient.

The steady state concentration of the oligomeric radical is given by:

$$[\mathbf{IM}^\bullet] = \frac{2k_d[\mathbf{I-I}]}{k_{p, \text{aq}}^1 C_w + k_{t, \text{aq}} T_R} \quad (4.8)$$

$$[\mathbf{IM}_i^\bullet] = \frac{k_{p, \text{aq}}^{i-1} C_w [\mathbf{IM}_{i-1}^\bullet]}{k_{p, \text{aq}}^i C_w + k_{t, \text{aq}} T_R} \quad (2 \leq i \leq z-1) \quad (4.9)$$

where T_R is the total concentration of radicals in the aqueous phase able to undergo termination reactions. As an extension to previous models,⁹ this term includes exited radicals:

$$T_R = [\mathbf{E}] + \sum_{i=1}^{j_{\text{crit}}-1} [\mathbf{IM}_i^\bullet] \quad (4.10)$$

Once the oligomeric radical becomes surface active, however, the complexity of the reaction scheme increases with micellar entry and particle entry being added to the possible events. Taking the rate coefficients for the entry of an i -mer into a particle to be k_e^i , the steady state concentration used in previous work⁵ may be extended to include micellar entry (with rate coefficient $k_{e, \text{micelle}}^i$):

$$[\mathbf{IM}_i^\bullet] = \frac{k_{p, \text{aq}}^{i-1} C_w [\mathbf{IM}_{i-1}^\bullet]}{k_{p, \text{aq}}^i C_w + k_{t, \text{aq}} T_R + k_e^i N_c + k_{e, \text{micelle}}^i [\text{micelle}]} \quad (z \leq i \leq j_{\text{crit}}-1) \quad (4.11)$$

As mentioned previously, it is possible to calculate the concentration of each of these radical species iteratively. To do so, an initial estimate for T_R is required and it has been found that a suitable starting point is to assume that particle and micelle entry events do not occur, giving:⁵

$$T_R = \sqrt{\frac{2k_d[\mathbf{I}]}{k_{t, \text{aq}}}} \quad (4.12)$$

A suitable convergence criterion may then be placed on the total radical concentration.

4.1.2.2 Entry Rate Coefficients

In the description of micellar entry and aqueous phase kinetics presented so far, the entry rate coefficients have remained undefined. For the purposes of this model, it is

assumed that the oligomeric radicals and the particles or micelles being entered have no interaction potential between them. The Smoluchowski diffusion model may thus be used to describe the entry rate coefficients.⁵ Experimental evidence for diffusion control of particle entry has been reported by Morrison *et al.*¹²

In the case of micellar entry, the entry rate coefficient is given by:

$$k_{e,\text{micelle}}^i = 4\pi D_i r_{\text{micelle}} N_A \quad (4.13)$$

where r_{micelle} is the radius of the surfactant micelle and D_i is the diffusion coefficient of an i -mer in the aqueous phase. In this study, D_i is taken to follow the ‘‘Rouse Model’’:^{5,13}

$$D_i = \frac{D_w}{i} \quad (4.14)$$

which assumes that the polymeric radical is in a rod-like conformation with D_w being the diffusion coefficient of the monomeric radical in water.

Similarly, the entry rate coefficients for entry of oligomeric radicals into particles may be defined as:⁵

$$k_e^i = 4\pi D_i r_s N_A \quad (4.15)$$

and the entry rate coefficient for the entry of an exited radical into a particle is given by:

$$k_e^E = 4\pi D_w r_s N_A \quad (4.16)$$

One final term that is useful to introduce to the discussion is the pseudo-first order rate coefficient for entry of initiator fragments into particles, ρ_{init} . This quantity is simply defined as:

$$\rho_{\text{init}} = \sum_{i=z}^{j_{\text{crit}}-1} k_{eL}^i [\text{IM}_i^\bullet] \quad (4.17)$$

4.1.3 Kinetics of Particle Growth

In modelling the kinetics of particle growth for an emulsion polymerisation, two kinetic models are used: zero-one and pseudo-bulk kinetics. Which model more accurately describes the situation depends chiefly on the particle size and the monomer being used. For reasons discussed below, only zero-one kinetics are used in this model. A brief discussion of pseudo-bulk kinetics may be found in Appendix 2.

4.1.3.1 Zero-One Kinetics

Zero-one kinetics is so named from its assumption that pseudo-instantaneous termination of the growing polymer chain will occur should a second radical enter the particle, thus allowing only zero or one radicals in any individual particle. This condition may be expressed in kinetic terms as meaning that termination is not rate determining.⁵ The validity of this model is now well tested experimentally¹⁴ and for many small particles its conditions are met.⁵ In this model, zero-one kinetics are utilised to simulate the growth of any secondary particles in the system.

Previous models of zero-one systems simply accounted for the number of particles with one radical or without any radicals.^{1,5} As in this study, more recent highly developed models⁷ have accounted for three separate populations: the number concentration of particles with no radicals, N_0 ; the number concentration of particles with one *polymeric* radical, N_1^p ; and the number concentration of particles with one *monomeric* radical, N_1^m . This allows chain transfer to monomer events to be successfully included, permitting the incorporation of exited monomeric radicals into the model.

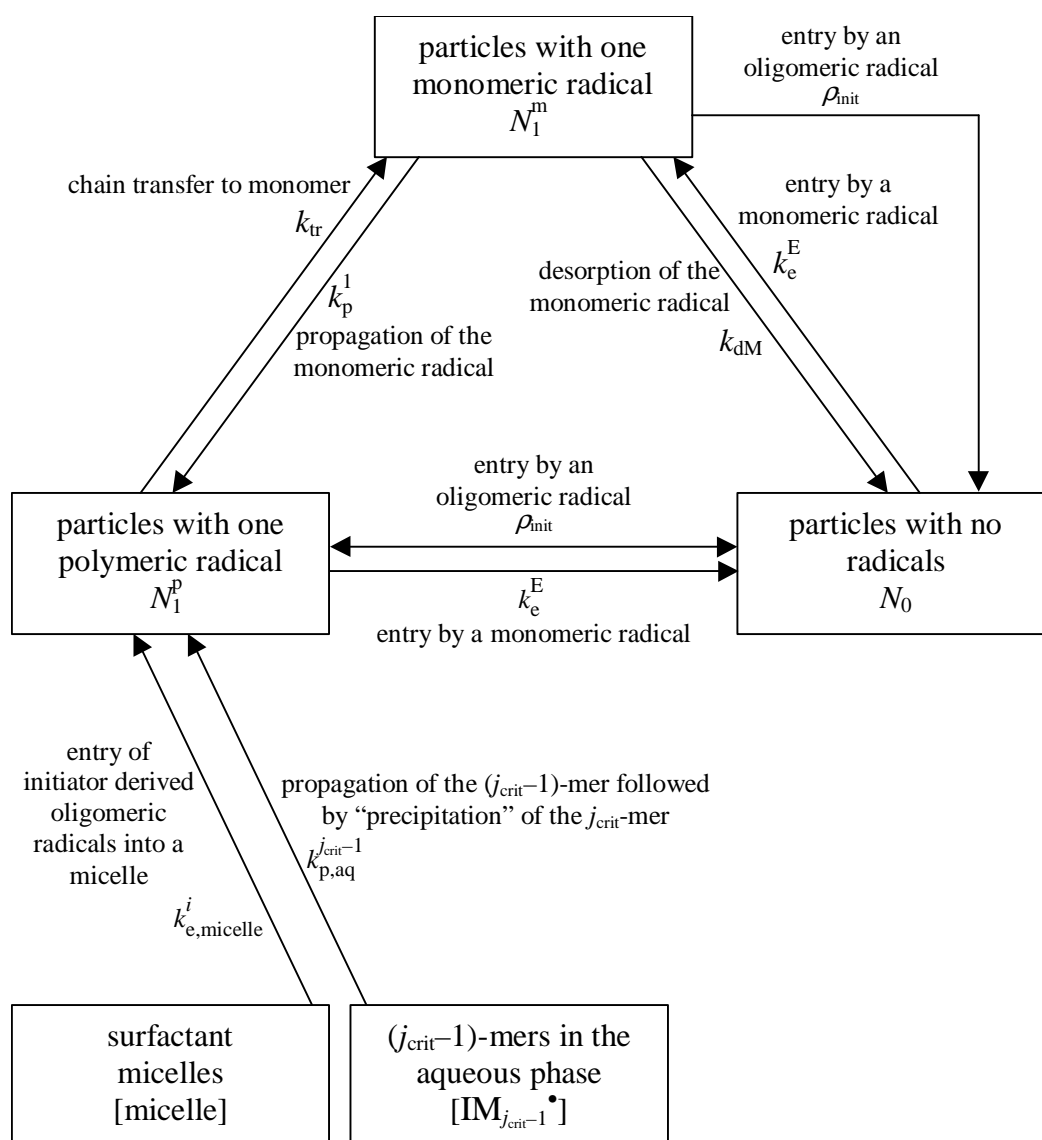


Figure 4.1: An illustration of the processes by which particles are formed and converted between particle types in a zero-one system. The populations and rate coefficients for these processes are included.

It is useful to consider the relationship between these three populations in pictorial form as shown in Figure 4.1. Here, each of the processes that contribute to the conversion of one particle to another are described along with the process of particle formation. It should be noted that since the concentration of exited radicals, E , is small, termination between a re-entering monomeric radical and a monomeric radical already in a particle is considered to be negligible.

From this pictorial representation, it is possible to construct the following differential equations that describe the population of the three types of particle being considered:

$$\frac{dN_0}{dt} = (\rho_{\text{init}} + k_e^E[\text{E}]) (N_1^p + N_1^m - N_0) \quad (4.18)$$

$$\begin{aligned} \frac{dN_1^p}{dt} = & \rho_{\text{init}}N_0 - (\rho_{\text{init}} + k_e^E[\text{E}])N_1^p - k_{\text{tr}}C_pN_1^p + k_p^1C_pN_1^m \\ & + k_{\text{p, aq}}^{\text{crit}-1}[\text{IM}_{j_{\text{crit}}-1}^\bullet]C_w + k_{\text{e, micelle}}[\text{micelle}] \end{aligned} \quad (4.19)$$

$$\frac{dN_1^m}{dt} = k_e^E[\text{E}]N_0 + k_{\text{tr}}C_pN_1^p - N_1^m(\rho_{\text{init}} + k_{\text{dM}} + k_p^1C_p) \quad (4.20)$$

where each of the rate coefficients has been described in detail in previous sections with the exception of the rate coefficient for the desorption of a monomeric radical, k_{dM} . Expressing this as a diffusive process gives:^{5,11}

$$k_{\text{dM}} = \frac{3D_wC_w}{r_s^2C_p} \quad (4.21)$$

As noted previously, the concentration of exited radicals is small and since propagation is fast once an exited radical enters a particle, the number of particles with one monomeric radical is also small. The steady state approximation may thus be used to calculate the number concentration of this species as:

$$N_1^m = \frac{k_e^E[\text{E}]N_0 + k_{\text{tr}}C_pN_1^p}{\rho_{\text{init}} + k_{\text{dM}}N_1^m + k_p^1C_p} \quad (4.22)$$

The average number of radicals per particle, \bar{n} , determines the overall rate of conversion from monomer to polymer in the system. In a zero-one system it may be expressed as a function of the number concentration of particles described above:

$$\bar{n} = \frac{N_1^p + N_1^m}{N_1^p + N_0 + N_1^m} \quad (4.23)$$

where the number concentration of particles with one monomeric radical, N_1^m , is small compared to the number of particles with polymeric radicals, N_1^p , and may thus be neglected, giving

$$\bar{n} \approx \frac{N_1^p}{N_1^p + N_0} \quad (4.24)$$

This is an important extension of previous models^{1,5} which assumed $\bar{n} = 1$ in calculating the amount of polymer formed.

The volume of polymer, v , produced in a zero-one system in which \bar{n} is constant may be written as a function of the molecular mass of the monomer unit, M_0 , and the density of the polymer, d_p :¹

$$v(t) = K \bar{n} t \quad (4.25)$$

where

$$K = k_p^{j_{\text{crit}}} C_p \frac{M_0}{N_A d_p} \quad (4.26)$$

It is assumed in this expression for K that the propagation rate coefficient for all polymeric radicals is the same as that of a j_{crit} -mer.

4.2 Avoiding New Nucleation – A Simple Model

It is important at this stage to return to the original motivation for modelling emulsion polymerisation – to determine the reaction parameters with which large polymer particles may be grown. This objective is equivalent to requiring that new nucleation does not occur since new particles formed during a reaction will grow in preference to the seed particles. This phenomenon is predicted by the theory presented above, where the rate of entry is proportional to r , but the rate of radius growth is proportional to r^{-3} . This has also been experimentally verified using competitive growth experiments.¹²

Constructing a complete model of particle growth, especially for large particles, is computationally difficult and subject to significant cumulative rounding errors. However, instead of performing simulations of *ab initio* experiments, it is possible to

undertake a series of seeded simulations and construct a time series solution by deconvoluting the reaction parameters used.

Implicit within this approach is the assumption that the population of particles is able to grow in any given simulation to form the “seed” for the next simulation. This approach may be justified by considering the relationship between the particle number, particle size and the mass of polymer, m_p :

$$m_p = \frac{4}{3}\pi r_s^3 N_c d_p V_{aq} \quad (4.27)$$

where V_{aq} is the volume of the aqueous phase.

From this mass balance, if the mass of polymer is increasing due to polymerisation reactions occurring then the particle size or particle number is increasing. Thus, if the particle number is not changing (i.e. secondary particle formation is not occurring, which is the “success” criterion for the reaction parameter) then the particles are able to grow. If the particles are able to grow, then they may become the “seed” particles for another binary assessment of the equivalent reaction parameters with a larger seed. In this way, a “seeded-series” approach with a number of snap-shots is generated which may be concatenated to make a complete *ab initio* reaction simulation.

In an optimised form (including the simplifications detailed below) it is possible to perform a large number of simulations using this model and the appropriate success criterion (see section 4.2.2) to evaluate whether the reaction parameters lead to a successful synthesis.

4.2.1 Simplifications in the Model

While there are quite complete models of emulsion polymerisation,^{6,7} they do not allow a large parameter space to be investigated in the method described above. This is due to the computational complexity of solving the equations of polymerisation over the entire particle size distribution. The most significant simplification in this

model is that the size distribution of the seed particles is taken to be infinitesimally narrow (a delta function) and that the particle size distribution (PSD, $n_r(r)$) of any new particles formed is similarly narrow:

$$n_r(r) = N_c^{\text{seed}} \delta(r - r_{\text{seed}}) + N_c^{\text{new}} \delta(r - r_{\text{new}}) \quad (4.28)$$

where the descriptors *new* and *seed* designate that the value pertains to the new and seed particles respectively.

This assumption is clearly unphysical, as all seeds have some polydispersity and new particle formation will occur over a period of time thus giving the secondary population considerable polydispersity. It will be seen in section 4.2.3.1 that the onset of significant secondary nucleation is so rapid that this simplification may be successfully made.

Further simplifications that are made in this model regard the process of particle formation. Droplet nucleation has been found to be unimportant in the styrene polymerisation and is accordingly omitted from this model. It is also assumed that all particles are stable, *i.e.* coagulation does not take place. This tends to cause the number concentration of new particles to be overestimated as seen in section 4.2.3.1.

It is well known that above the critical micelle concentration, cmc, micellar nucleation becomes significant.^{5,15} As a consequence, the simulations in this study are performed well below cmc to avoid ‘trivial’ secondary particle formation. This sets the concentration of micelles to zero, preventing micellar nucleation.

It is also assumed that the aqueous phase radicals are in a steady state permitting use of the Maxwell-Morrison model⁹ as outlined in section 4.1.2.1. Moreover, it is assumed that the propagation rate coefficients in the aqueous phase and in the particles are equal:

$$k_{p,\text{aq}}^i = k_p^i \quad (4.29)$$

The particle growth kinetics of any secondary particles is assumed to be zero-one in nature as initially they are small and small particles are typically zero-one.^{5,16} Moreover, recently developed models for determining the applicability of zero-one and pseudo-bulk growth kinetics indicate that small polystyrene is zero-one.^{7,14} This is also supported by experimental evidence.¹⁷

Finally, based on equation 4.21, it is assumed that the flux of exited radicals from the seed particles is insignificant, as these particles are large. This is an important simplification as it eliminates the need to simulate the particle growth kinetics for the large particles as these kinetics are no longer needed for particle growth (due to the “seeded-series” simulation technique) or to generate aqueous monomeric radicals. Since estimating the rate of radical exit from a pseudo-bulk system is quite difficult,^{6,7} this represents a significant computational saving.

4.2.2 Implementation of the Model

The implementation of the model detailed above was undertaken using a differential equation solving algorithm developed by Gear.¹⁸

4.2.2.1 Final Form of the Mathematical Model

With the simplification of the particle size distribution described in equation 4.28 and the steady state approximation for the aqueous phase radicals, the model may be reduced to three differential equations: 4.18, 4.19 and:

$$\frac{d[E]}{dt} = k_{dM}^{new} N_1^m - k_{t,eq}^{E,new} [E] N_c^{new} - k_{t,eq} T_R \quad (4.30)$$

It should be noted that it is necessary to rewrite the equations for the steady state concentration of aqueous phase radicals (equation 4.11) in terms of the bimodal particle size distribution of equation 4.28:

$$[IM_i \bullet] = \frac{k_{p,eq}^{i-1} C_w [IM_{i-1} \bullet]}{k_{p,eq}^i C_w + k_{t,eq} T_R + k_{t,eq}^{i,new} N_c^{new} + k_{t,eq}^{i,seed} N_c^{seed}} \quad (z \leq i \leq j_{crit}-1) \quad (4.31)$$

For completeness, it is also necessary to re-express the entry rate coefficients for the oligomeric radicals and exited radicals (equations 4.15 and 4.16) in terms of the particles being entered:

$$k_{\text{e}}^{i,\text{new}} = 4\pi D_i r_s^{\text{new}} N_A \quad (4.32a)$$

$$k_{\text{e}}^{i,\text{seed}} = 4\pi D_i r_s^{\text{seed}} N_A \quad (4.32b)$$

$$k_{\text{e}}^{\text{E,new}} = 4\pi D_w r_s^{\text{new}} N_A \quad (4.33a)$$

$$k_{\text{e}}^{\text{E,seed}} = 4\pi D_w r_s^{\text{seed}} N_A \quad (4.33b)$$

Thus the pseudo-first order rate coefficient for the entry of initiator fragments into the particles (equation 4.17) must also differentiate between the particles being entered:

$$\rho_{\text{init}}^{\text{new}} = \sum_{i=z}^{j_{\text{crit}}-1} k_{\text{e}}^{i,\text{new}} [\text{IM}_i \bullet] \quad (4.34a)$$

$$\rho_{\text{init}}^{\text{seed}} = \sum_{i=z}^{j_{\text{crit}}-1} k_{\text{e}}^{i,\text{seed}} [\text{IM}_i \bullet] \quad (4.34b)$$

4.2.2.2 Input Parameters Used by the Model

In a seeded emulsion polymerisation experiment with a given monomer (in this case styrene) the principal reaction parameters are the seed particle number and size, the initiator concentration and the reaction temperature.

Of these parameters, the temperature dependence is the most complex as each of the physical rate coefficients would vary. For the purposes of this study, the temperature was maintained at 50 °C, while the other parameters were varied over the range described in Table 4.1. It should be noted that the lowest value of the initiator concentration used in this parameter space has been found to be less than the level of thermal initiation.^{17,19,20}

Table 4.1: The parameter space of initiator concentration, particle concentration and seed radius over which the simulations were performed.

parameter	minimum value	maximum value
[initiator]	10^{-6} M	10^1 M
N_c^{seed}	10^{12} dm ⁻³	10^{16} dm ⁻³
r_{seed}	20 nm	5000 nm

The remaining physical data required to perform the calculations described in this chapter are shown in Table 4.2.

Table 4.2: The parameters used for the modelling in this study of styrene polymerisation with a persulfate initiator at 50 °C.

parameter	value	reference
k_d	10^{-6} s ⁻¹	21
k_p^1	1040 dm ³ mol ⁻¹ s ⁻¹	5
$k_p^i, i > 1$	260 dm ³ mol ⁻¹ s ⁻¹	17,22
$k_{t,\text{aq}}$	10^9 dm ³ mol ⁻¹ s ⁻¹	1
k_{tr}	9.3×10^{-3} dm ³ mol ⁻¹ s ⁻¹	23
$C_w = C_w^{\text{sat}}$	4.3×10^{-3} mol dm ⁻³	24
$C_p = C_p^{\text{sat}}$	5.5 mol dm ⁻³	17
z	3	9
j_{crit}	5	9
D_w	1.5×10^{-5} cm ² s ⁻¹	25
d_p	1.044 g cm ⁻³	17

Finally, the time after which the degree of new nucleation was measured was set to 1200 s of model time, with a time-step of 0.01 s for the Gear algorithm.¹⁸ Consideration of the numerical derivative of the particle number indicates that after a

short period of time all particle formation becomes a function of numerical noise (due to the finite precision of the computations being performed).

The time-step over which the Gear differential algorithm was used is the step-value at which the results of the modelling were independent of the step-value. More precisely, this is the value for the time-step at which point halving the time-step did not produce a significant effect on the output.

4.2.3 Comparison with Experiment and Other Models

To determine the accuracy of the model, it is useful to compare the results of the simulations with experimental data and other more complete models. The comparisons below are only for relatively small particles, as this is the range over which independent experiments and numerical simulations have been performed.

4.2.3.1 Comparison with Experiment

Very little experimental data quantifying the degree of new nucleation in styrene systems is available, particularly for large particles. For smaller particles (less than 300 nm in radius) some experimental data has been collected. The details of these experiments are reported by Morrison and Gilbert.¹

The number concentration of particles used was varied as shown in Figure 4.2. The degree of new nucleation was measured by counting the number of small and large particles using transmission electron microscopy, with the results expressed as a ratio between the number of new particle formed and the number of pre-existing particles in the experiment (*new:old*).

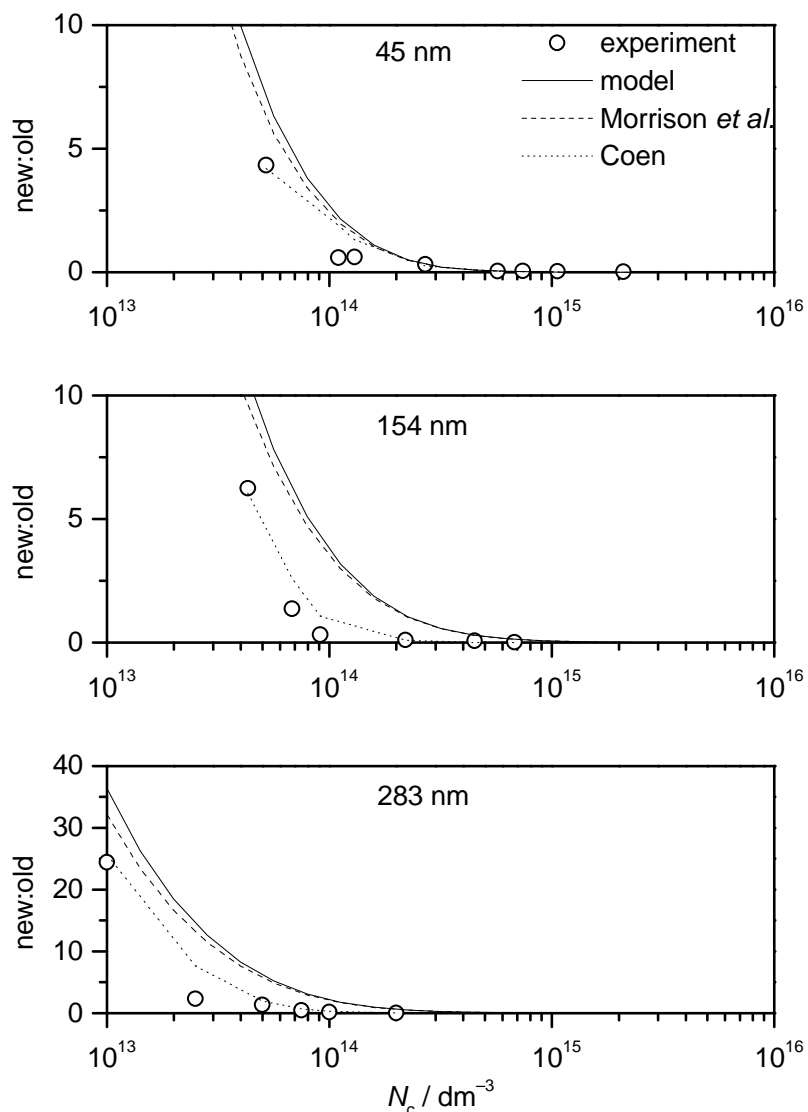


Figure 4.2: A comparison between the model used in this study and other models for small particle sizes. The original experimental data (open circles) is that of Morrison and Gilbert,¹. The solid line is based on this work, the dashed line on the model proposed by Morrison and Gilbert,¹ and the dotted line the work of Coen.⁷ The data are expressed as the ratio of the number of new particles formed in the reaction to the number of pre-existing particles. A comparison of the models represented in this figure may be found in section 4.2.3.2.

From Figure 4.2 it is evident that the onset of new nucleation is rapid as the number concentration of the seed particles is reduced. Moreover, it is seen that the model is able to reproduce the experimental data with reasonable agreement. The rapid onset of secondary nucleation may be described as a *catastrophe*.

Until further nucleation studies are undertaken, particularly for larger particles, the limit of the verification of this model with respect to experimental data has been reached.

4.2.3.2 *Comparison with Other Models*

This model is found to produce quite similar results to other models for small particle sizes as shown in Figure 4.2. In the case of the modelling performed by Morrison and Gilbert,¹ the particle kinetics were not simulated (hence it was assumed that $\bar{n} = 1$) and chain transfer to monomer was not included. It is found that the principal difference between the two models is due to the particle size being smaller due to slower growth from a reduced, physically reasonable \bar{n} . From Equation 4.25, the reduction in \bar{n} causes the new particles in this model to grow more slowly than those in the model of Morrison and Gilbert.¹ This reduces the rate of oligomeric radical capture and allows increased homogeneous nucleation.

Comparison with a more complete model⁷ of the emulsion polymerisation process compares favourably with these samples. It should be noted however, that the particle number is overestimated in this model, as the small, secondary particles are not permitted to coagulate as in the more complete model. It is also interesting to observe that if the seed latex were polydisperse then the particle size distribution assumptions contained in this model (see section 4.2.1) would make the results inherently unreliable.

While the degree to which this model is seen to agree with other more complete models is favourable, it must be noted that this is only a binary assessment tool and not a tool for predicting the final particle size distribution. It should be realised that the model proposed by Morrison and Gilbert¹ is quite similar in its physical assumptions to this model and that the accuracy of the predictions of the degree of new nucleation was rationalised in terms of a strong dependence on the number concentration of the seed.

It should also be noted that the model appears to overestimate the degree of secondary nucleation, which may have implications for the uses outlined in section 4.2.4. The onset of secondary nucleation is so rapid, however, that the use of the model as a predictive tool is justified. Furthermore, since it is intended to use this model to avoid secondary nucleation, this is not a serious shortcoming.

4.2.4 The Model as a Predictive Tool

The use of this model as predictive tool for determining the success or otherwise of a set of experimental conditions in avoiding secondary nucleation was the original goal of this section of the study. A series of over 27,000 simulations was performed over the parameter space described in Table 4.1 and using the method described in section 4.2.2. As in previous studies,^{1,7} these data were expressed as the ratio of the number of new particles formed during the reaction to the number of pre-existing particles. The data were interpreted using scientific visualisation software described in Appendix 3, the output from which is shown in Figures 4.3 and 4.4.

With reference to the experimental methods of determining whether or not new nucleation has occurred in an experiment, it may be seen that it is reasonable to set an upper limit for the value of *new:old* for an experiment to be considered “successful”. The practical limit of transmission electron microscopy for detecting new nucleation in an experiment is around one new particle per 100 pre-existing particles, and this value is taken as the limit for these simulations. Using this success criterion, a surface in the parameter space of initiator concentration, particle size and particle number concentration where new nucleation becomes detectable (*new:old* = 0.01) may be drawn. This is depicted in Figure 4.3, where it may be seen that above this surface, new nucleation is considered to be insignificant while below the surface it is significant.

The colour scheme superposed onto the surface shown in Figure 4.3 indicates the solids fraction of the latex. This is an important practical consideration, as it is

generally considered that 40-50% solids is a practical upper limit for monodisperse latices in the emulsion polymerisation of styrene. It should be noted that the surface has been removed (more strictly made transparent) at solids fractions in excess of 50%.

The edge of this surface may be seen as the upper limit to the synthesis of large particles by aqueous initiated emulsion polymerisation. When it is recalled that the lowest initiator concentrations used here (10^{-6} mol dm⁻³) are below thermal initiation levels (see section 4.2.2.2) the practical upper limit as seen in Figure 4.3 is reduced.

While the three-dimensional representation shown in Figure 4.3 provides a useful overview of the results, it is often difficult to quantify the results on the basis of such a rendering. To this end, a contour map, as shown in Figure 4.4, provides considerably more detail. It should be noted that in both Figures 4.3 and 4.4, the square blocks that may be seen at the “large particle size”-end of the surface are an artefact of the visualisation process.

With reference to the nature of the strong dependence of the degree of new nucleation on the particle number discussed in section 4.2.3, this surface may be described as a “catastrophe surface” across which the results of an experiment change dramatically. This allows interpretation of these results in terms of the suitability of emulsion polymerisation to the synthesis of large particles for use in Chemical Force Microscopy.

It may be seen from Figure 4.4 that the synthesis of particles with a radius in excess of 1 μm requires quite high solids fractions. Such experimental conditions have been observed to lead to coagulation and unsuccessful experiments. Moreover, an effective upper limit on the size of particles produced by these methods is found to be 2 μm (radius). Such a recipe would be quite slow, as the initiator concentration is low. Further, its end point is close to the catastrophe so it would be prone to failure due to local inhomogeneity.

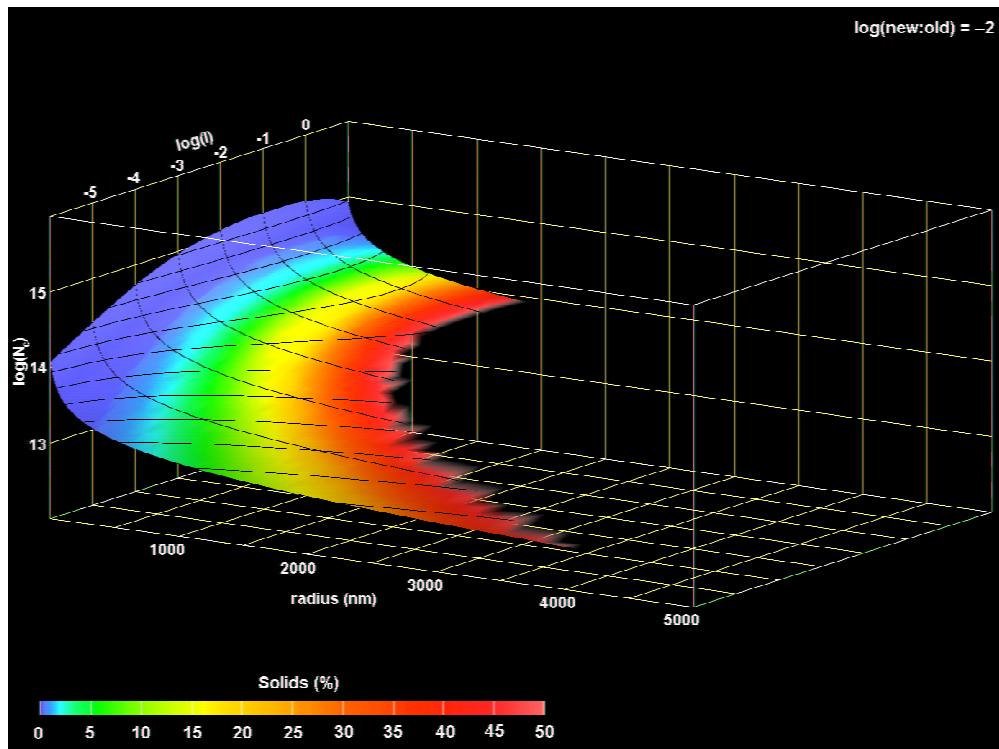


Figure 4.3: A surface of constant *new:old* in the parameter space of initiator concentration, particle size and particle number concentration. The colour scheme indicates the solids fraction of the reaction over the range 0-50%.

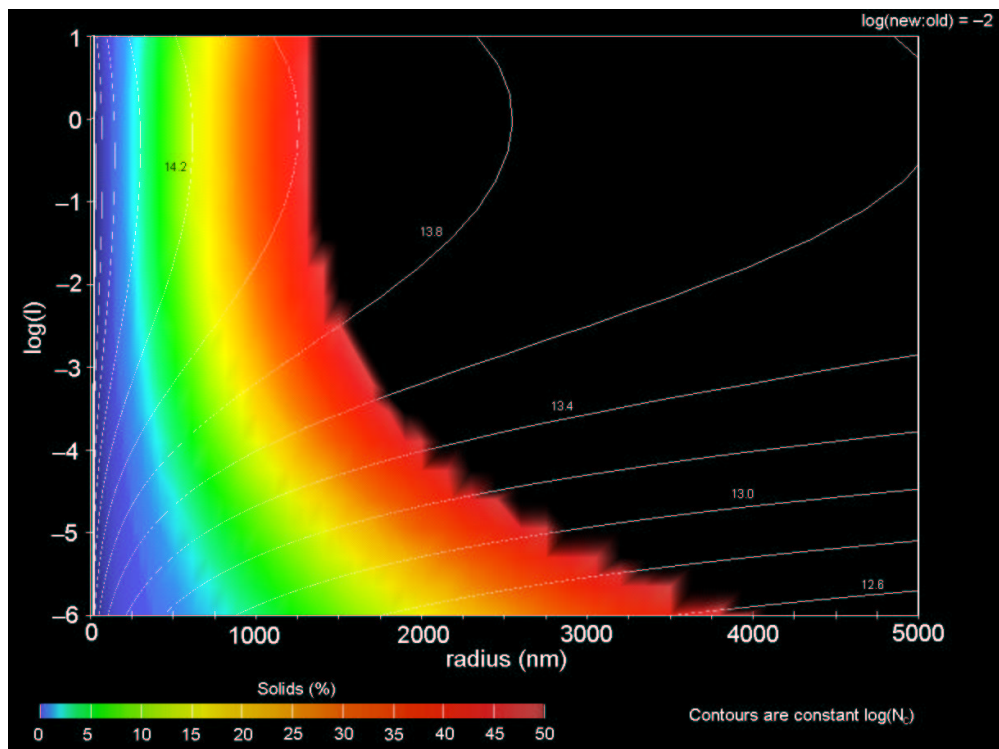


Figure 4.4: The surface shown in Figure 4.3 re-expressed as a contour plot, where the contour lines indicate constant particle number concentration.

The conclusion that may be drawn from this work is that emulsion polymerisation with an aqueous phase initiator is unsuitable for Chemical Force Microscopy as it is not possible to generate particles of the required size. While it may still be possible to graft surface modifications to the particles by an emulsion polymerisation technique, these results indicate that this process would also be difficult.

References

1. B.R. Morrison and R.G. Gilbert, *Macromolecular Symposia*, **92**, 13-30 (1995).
2. Y. Chung-li, J.W. Goodwin, and R.H. Ottewill, *Progr. Colloid Polym. Sci.*, **60**, 163-175 (1976).
3. J.W. Goodwin, J. Hearn, C.C. Ho, and R.H. Ottewill, *Colloid Polym. Sci.*, **252**, 464-471 (1974).
4. J.W. Goodwin, R.H. Ottewill, and R. Pelton, *Colloid Polym. Sci.*, **60**, 163-175 (1979).
5. R.G. Gilbert, *Emulsion Polymerization: A Mechanistic Approach*, (Academic, London, 1995).
6. E.M. Coen and R.G. Gilbert, in *Polymeric Dispersions. Principles and Applications*, edited by J.M. Asua (Kluwer Academic, Dordrecht, 1997), **NATO Advanced Studies Institute**, page 67-78.
7. E.M. Coen, PhD thesis, University of Sydney (1999).
8. P.A. Clay and R.G. Gilbert, *Macromolecules*, **28**, 552-69 (1995).
9. I.A. Maxwell, B.R. Morrison, D.H. Napper, and R.G. Gilbert, *Macromolecules*, **24**, 1629 (1991).

10. R.M. Fitch and C.H. Tsai, in *Polymer Colloids*, edited by R.M. Fitch (Plenum, New York, 1971), page 73.
11. J. Ugelstad and F.K. Hansen, *Rubber Chem. Technol.*, **49**, 536 (1976).
12. B.R. Morrison, I.A. Maxwell, R.G. Gilbert, and D.H. Napper, in *ACS Symp. Series - Polymer Latexes - Preparation, Characterization and Applications*, edited by E.S. Daniels, E.D. Sudol, and M. El-Aasser (American Chemical Society, Washington D.C., 1992), ACS Symposium Series **492**, page 28-44.
13. J.D. Ferry, *Viscoelastic Properties of Polymers*, 2nd (Wiley-Interscience, New York, 1980).
14. S. Maeder and R.G. Gilbert, *Macromolecules*, **31**, 4410-8 (1998).
15. N. Sütterlin, in *Polymer Colloids II*, edited by R.M. Fitch (Plenum, New York, 1980),
16. B.S. Casey, B.R. Morrison, I.A. Maxwell, R.G. Gilbert, and D.H. Napper, *J. Polym. Sci. A: Polym. Chem.*, **32**, 605-30 (1994).
17. B.S. Hawkett, D.H. Napper, and R.G. Gilbert, *J. Chem. Soc. Faraday Trans. 1*, **76**, 1323 (1980).
18. C.W. Gear, *Numerical Initial Boundary Value Problems in Ordinary Differential Equations*, (Prentice-Hall, New York, 1971).
19. P.A.G.M. Scheren, G.T. Russell, D.F. Sangster, R.G. Gilbert, and A.L. German, *Macromolecules*, **28**, 3637-49 (1995).
20. M.E. Adams, G.T. Russell, B.S. Casey, R.G. Gilbert, D.H. Napper, and D.F. Sangster, *Macromolecules*, **23**, 4624 (1990).
21. I.M. Kolthoff and I.K. Miller, *J. Am. Chem. Soc.*, **73**, 3055 (1951).

22. M. Buback, L.H. Garcia-Rubio, R.G. Gilbert, D.H. Napper, J. Guillot, A.E. Hamielec, D. Hill, K.F. O'Driscoll, O.F. Olaj, J. Shen, D. Solomon, G. Moad, M. Stickler, M. Tirrell, and M.A. Winnik, *J. Polym. Sci., Polym. Letters Edn.*, **26**, 293-297 (1988).
23. A.V. Tobolsky and J. Offenbach, *J. Polym. Sci.*, **16**, 311 (1955).
24. W.H. Lane, *Ind. Eng. Chem.*, **18**, 295 (1946).
25. C.R. Wilke and P. Chang, *A.I.Ch.E. J.*, **1**, 264 (1955).